IFSCC 2025 full paper (IFSCC2025-570)

100-day extended-time cultured in vitro 3D skin model mimicking chronological aging for studying long term repeated topical application of a cosmetic product

Shalina Hassanaly[1], Morgan Dos Santos[2], Kilian Laho[2], Julie Rorteau[2], Amélie Thépot[2], Françoise Vannier[1], Auriane Flais-Ferreira[1], Jean-Christophe Choulot[1], Mathilde Thomas[3]

[1] Caudalie, Gidy, France
[2] Labskin Creations, Lyon, France
[3] Caudalie, Paris, France

1. Introduction

Skin ageing is a multifactorial biological process resulting from both intrinsic (chronological) and extrinsic (environmental) factors. While extrinsic ageing is largely driven by ultraviolet radiation, pollution, and oxidative stress, intrinsic ageing is governed by genetic programming and the progressive decline in cellular and tissue function over time **[1]**. Clinically and histologically, intrinsic ageing is characterised by epidermal thinning, impaired barrier function, and extracellular matrix (ECM) remodelling, including fragmentation and reduced synthesis of elastin and fibrillin-1 fibres **[2,3]**.

Over the past few decades, various *in vitro* models have been developed to investigate the mechanisms of skin ageing and to evaluate the efficacy of anti-ageing active ingredients. Among these, reconstructed human epidermis (RHE) models are widely used due to their simplicity and ability to reproduce stratified epidermal layers. However, as RHEs are composed exclusively of keratinocytes and lack a dermal compartment, they are inadequate for studying dermal remodelling, fibroblast/ECM interactions, or other processes central to intrinsic ageing. More advanced full-thickness three-dimensional skin equivalents (SEs) offer improved physiological relevance by incorporating both epidermal and dermal components, more closely mimicking native skin architecture. Nevertheless, most of these models are cultured for relatively short periods (21–42 days), which limits their relevance for studying the progressive nature of chronological ageing **[4]**.

A key challenge in skin tissue engineering lies in reconstructing a dermis that is physiologically relevant, mechanically stable, and capable of supporting appropriate epidermal differentiation, ECM remodelling, and long-term viability. Conventional approaches, such as the Bell model, rely on a collagen I gel lattice seeded with fibroblasts **[5]**. While widely used, this type of matrix lacks mechanical stability, tends to compact over time, and does not replicate the porous architecture or biomechanical properties of native dermal ECM. These limitations restrict long-term culture and can lead to poor nutrient diffusion, excessive contraction, and non-physiological fibroblast behaviour **[6]**. They also limit the timeframe available for testing active ingredients, particularly those requiring repeated application or targeting slow-onset biological processes such as intrinsic ageing.

To mimic aged skin *in vitro*, several strategies have been proposed. These include the use of replicative senescence, typically induced by repeated passaging of dermal fibroblasts until they reach the Hayflick limit, a method shown to induce key ageing markers such as $p^{16INK4a}$ expression, reduced collagen synthesis, and increased matrix degradation **[7,8]**. While this approach effectively models cellular senescence, it remains dependent on artificially aged cells and does not replicate the time-dependent, cumulative ageing process that occurs *in vivo*. Other models rely on progerin overexpression or telomerase inhibition **[9,10]**, but these methods can lead to unphysiological or unstable tissue phenotypes. Furthermore, many of these systems lack reproducibility, fail to develop full tissue-level ageing features, or are unsuitable for long-term topical treatment studies.

To address these limitations and enable the evaluation of long-term cosmetic product application, we employed a full-thickness 3D *in vitro* skin model maintained in culture for an extended period of 100 days, allowing the tissue to age progressively under standard conditions, without genetic manipulation or accelerated cellular senescence **[6]**. This model is based on a chitosan-crosslinked collagen glycosaminoglycan (GAG) scaffold, which is seeded with primary human fibroblasts and overlaid with human keratinocytes to form a fully differentiated epidermis. Unlike senescence-based models, this long-term approach allows the gradual emergence of ageing-related phenotypes, including epidermal thinning, reduced barrier protein expression, and ECM degradation, in a dynamic and reproducible manner. Importantly, it also enables repeated topical application of cosmetic formulations, closely mimicking real-life usage patterns.

In this study, we describe for the first time the use of this model to assess the anti-ageing efficacy of a cosmetic formulation applied biweekly over a 58-day period, with a particular focus on ECM-related outcomes in the dermis.

2. Materials and Methods

2.1 Ethical considerations and human cutaneous cell isolation

Human skin tissues were collected from surgical waste from anonymous healthy donors. Surgical residues were anonymised, and written informed consent was obtained from the patients in accordance with the ethical guidelines from Lyon University Hospital (Hospice Civils de Lyon) and approved by ethical committee of the Hospices Civils de Lyon according to the principles of the Declaration of Helsinki and Article L. 1243-4 of the French Public Health Code. The skin samples used in this study were part of a declared human tissue collection (Declaration No. DC-2024-6232) registered with the French Ministry of Research and held by LabSkin Creations (Lyon, France). Primary cultures of human dermal fibroblasts and epidermal keratinocytes were established from healthy skin biopsies obtained from infant donors (<5 years old).

2.2 3D full-thickness reconstructed model and cosmetic treatment

To assess the anti-ageing efficacy of a cosmetic formulation, we novel evaluation protocol was developed using an *in vitro* 3D full-thickness skin ageing model. This skin equivalent (SE) was engineered with primary human fibroblasts cultivated into a unique porous scaffold made of chitosan-cross-linked collagen glycosaminoglycan polymer on top of which were subsequently seeded human keratinocytes to form a stratified epidermis. To mimic chronological aging, the cultivation time of the skin equivalent model was extended from 37 to 100 days, allowing the evaluation of repeated application of skin care products. Throughout this period, the cosmetic product was topically applied twice a week. For each cell culture condition, 3D skin equivalents were generated in triplicate. After 37, 75 and 100 days of culture, tissues were harvested, fixed in neutral buffered formalin 4% (Diapath) for 24 hours and embedded in paraffin. Paraffin-embedded samples were cut into sections of 5µm.

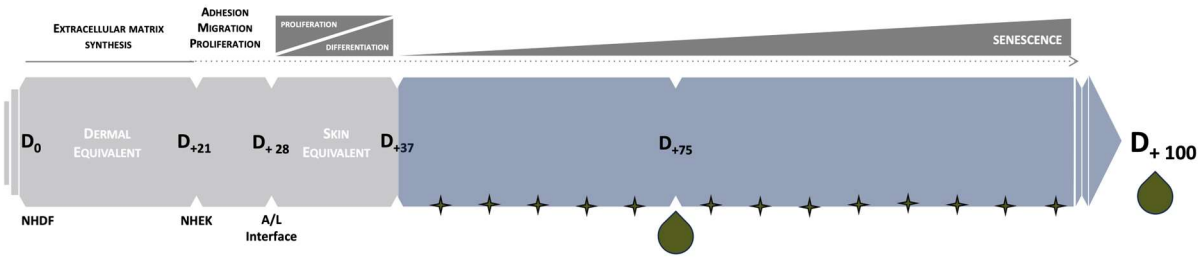

Figure 1. Skin tissue engineering strategy and product application methodology.

2.3. Histological analysis

To evaluate the global skin architecture of the samples, haematoxylin-phloxin-saffron (HPS) staining was performed. Paraffin sections of 5µm of each condition were cut. After dewaxing and rehydration, the samples were stained HPS. After rinsing, the sections were dehydrated before the mounting of the slides with a hydrophobic mounting medium.

2.4 Immunohistological analysis

For immunofluorescence analysis on paraffin sections, heat-mediated antigen retrieval was performed, followed by blocking with PBS containing 4% BSA. Sections were incubated overnight at room temperature with primary antibodies targeting filaggrin, loricrin, cytokeratin-10, fibrillin-1, and elastin (diluted in PBS/BSA 4%). After rinsing, sections were incubated for 1 hour with Alexa Fluor 488- or 568-conjugated anti-mouse or anti-rabbit secondary antibodies (Molecular Probes, Invitrogen). Nuclei were counterstained with DAPI. Negative controls were included by replacing the primary antibody with isotype-matched IgG.

2.5 Image acquisition

HPS-stained and immunostained tissue sections were imaged using an Axio Observer A1/D1 optical microscope (Zeiss). Images were acquired with an AxioCam HRc camera and processed using ZEN 2 Pro software (Zeiss). For each condition, nine representative images were captured under identical settings.

2.6 Tissue morphometry analysis

Epidermal thickness was quantified from HPS-stained images using a Euclidean distance map. Epidermal pixels were segmented, and 8-bit binary images were converted into 16-bit distance maps. The basal epidermal line was identified and used to compute the mean distance to the *stratum corneum*, representing the epidermal thickness in micrometres (µm).

For immunofluorescence markers, positive areas (red or green signal) were automatically segmented from background pixels. Images were binarised, processed using morphological operators, and sieved to isolate regions of interest. The surface area of positive signal was measured and normalised to either the epidermal or dermal thickness, depending on the marker. Results were expressed as the percentage of positive area.

2.7 *Statistical analysis*

Statistical analyses were performed using R software (R Foundation for Statistical Computing, Vienna, Austria). Data normality was assessed using the Shapiro–Wilk test. For normally distributed data, analysis of variance (ANOVA) was followed by pairwise t-tests as post hoc comparisons. For non-normally distributed data, the Kruskal–Wallis test was applied, followed by pairwise Wilcoxon–Mann–Whitney tests. Statistical significance was indicated as follows: $P < 0.05$ (*), $P < 0.01$ (**), and $P < 0.001$ (***).

3. Results

3.1 Progressive epidermal alterations induced by long-term culture

Histological and immunohistological analyses revealed that prolonged *in vitro* culture induced marked and progressive alterations in the epidermal compartment of the 3D SE (Figures 2 and 3). At day 37, haematoxylin-phloxin-saffron (HPS) staining showed a well-organised, pluristratified epidermis with distinct basal, spinous, granular, and cornified layers. As culture duration increased, structural degradation became evident. By day 75, the viable epidermis

displayed fewer cell layers, with signs of thinning and a less defined *stratum granulosum*. At day 100, these alterations were more pronounced, with a flattened and thinned epidermis, reduced stratification, and a disorganised *stratum corneum*. In parallel, the regularity of the dermal-epidermal junction decreased over time, suggesting impaired epidermal–dermal cohesion.

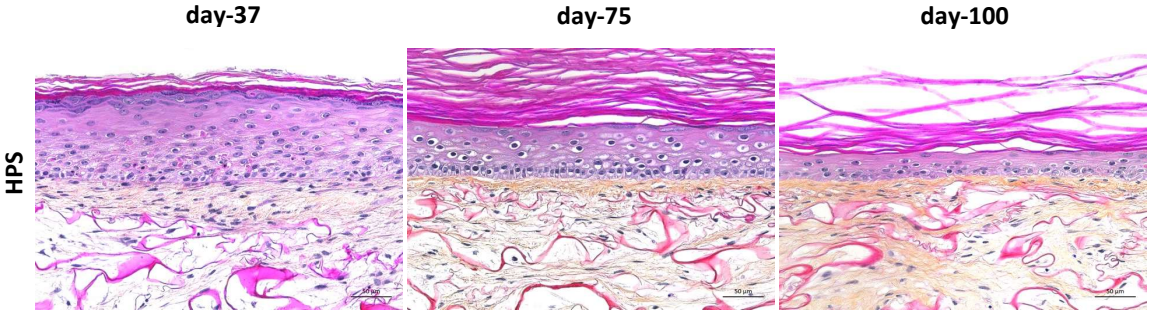

Figure 2. Histological changes in the epidermis during long-term culture of 3D SEs. Representative HPS-stained sections of 3D full-thickness skin equivalents at day 37, day 75, and day 100 of culture. Scale bar = 50 µm.

To support these morphological observations, expression of key epidermal differentiation markers, cytokeratin-10 (CK10), filaggrin, and loricrin, was assessed by immunofluorescence and quantified (Figure 3). At day 37, all three markers were abundantly and uniformly expressed in their expected epidermal layers. CK10 was strongly localised to suprabasal keratinocytes, while filaggrin and loricrin were clearly detected in the upper differentiating layers, reflecting robust terminal differentiation and barrier formation. At day 75, a decline in signal intensity and homogeneity was already noticeable for filaggrin and loricrin. By day 100, expression of all three markers was drastically reduced (Figure 3a).

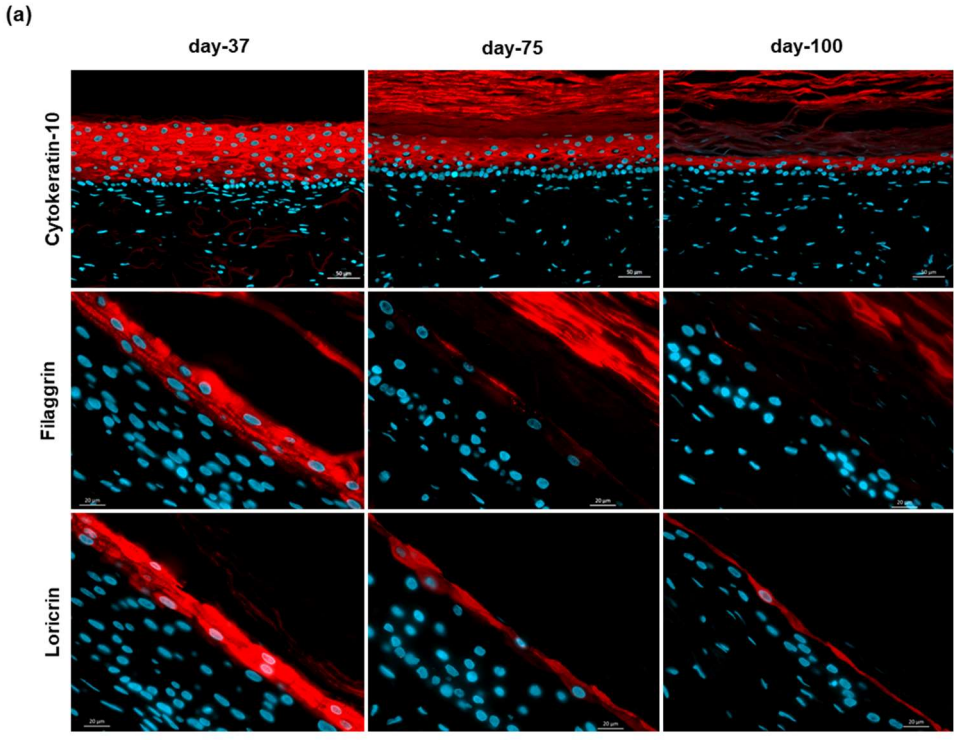

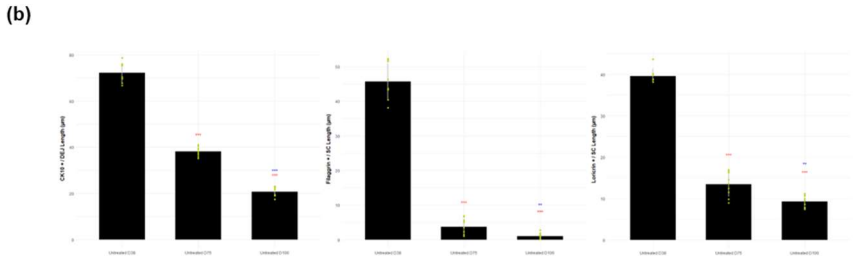

Figure 3. Decreased expression of epidermal differentiation markers during extended *in vitro* culture. **(a)** Representative images showing immunostaining of cytokeratin-10, filaggrin, and loricrin (red) in 3D SE cultured for 37, 75, and 100 days. Nuclei are counterstained with DAPI (blue). **(b)** Quantification of the percentage of positive surface area for each marker. Data are presented as mean ± SD. P < 0.05, P < 0.01, *P < 0.001. Scale bar = 50 µm.

Quantitative image analysis confirmed these observations: CK10 expression declined by ~60%, filaggrin by >85%, and loricrin by nearly 70% over the culture period (Figure 3b).

Altogether, these results demonstrate that extended culture induces both structural and molecular features of epidermal ageing in vitro, including epidermal thinning, impaired differentiation, and loss of barrier-related protein expression—mimicking hallmarks of intrinsic skin ageing.

3.2 Gradual disorganisation and fragmentation of the dermal elastic matrix during extended culture

To investigate the impact of long-term culture on dermal matrix integrity, we analysed the expression and organisation of two key components of the elastic fibre network, fibrillin-1 and elastin, using immunofluorescence staining (Figure 4). At day 37, fibrillin-1 (green) and elastin (red) were both abundantly expressed in the upper dermis, forming a dense and well-organised fibre network closely aligned along the dermal-epidermal junction. Co-localisation analysis confirmed structured and overlapping elastic microfibrils, indicative of a functional elastic scaffold.

By day 75, fibrillin-1 fibres remained detectable but appeared more loosely arranged, while elastin staining showed early signs of disorganisation. Notably, elastin fibres exhibited discontinuity, thinning, and partial fragmentation, suggesting the beginning of elastic network degradation. These structural alterations were further exacerbated by day 100, when both markers displayed markedly reduced signal intensity. Fibrillin-1 and elastin fibres appeared short, irregular, and highly fragmented, with disrupted alignment and weakened co-localisation at the dermal-epidermal junction.

Together, these findings indicate that the dermal compartment of the 3D SE undergoes progressive disorganisation of the elastic fibre network over time. The fragmentation and loss of structure in fibrillin-1 and elastin closely recapitulate age-related deterioration of the dermal ECM, further validating this long-term model as a relevant platform for studying intrinsic skin ageing.

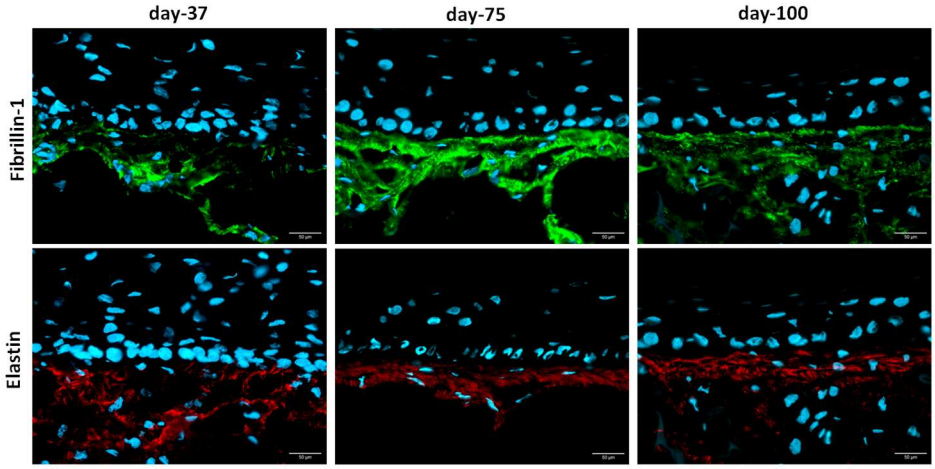

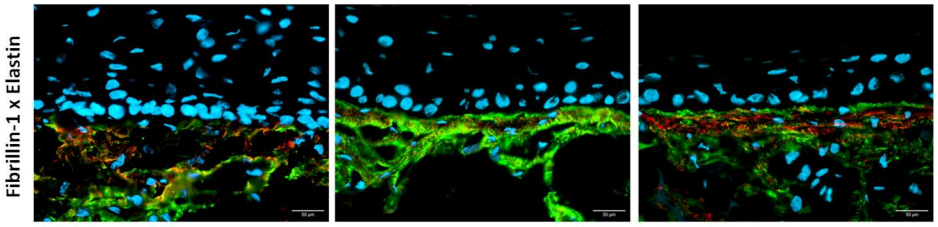

Figure 4. **Long-term culture induces degradation of dermal elastic fibre architecture in 3D SEs.** Representative images of fibrillin-1 (green) and elastin (red) immunostaining in the dermal compartment of 3D SE cultured for 37, 75, and 100 days. Nuclei are counterstained with DAPI (blue). Merged images highlight the loss of fibre co-localisation and architectural integrity over time. Scale bar = 50 µm.

3.3 Repeated topical application of the cosmetic product restores epidermal structure and differentiation

To evaluate the regenerative effect of the cosmetic formulation, the final product (FP) was topically applied twice weekly on 3D skin equivalents over a 58-day period. Histological and immunohistological analyses revealed a clear improvement in epidermal structure compared to untreated aged controls (Figure 5).

HPS staining (Figure 4a) showed that FP-treated tissues exhibited a thicker and more stratified epidermis, particularly at day 100, where untreated controls displayed pronounced thinning. Quantification confirmed that epidermal thickness was increased by 112% following treatment, indicating a significant recovery of epidermal architecture.

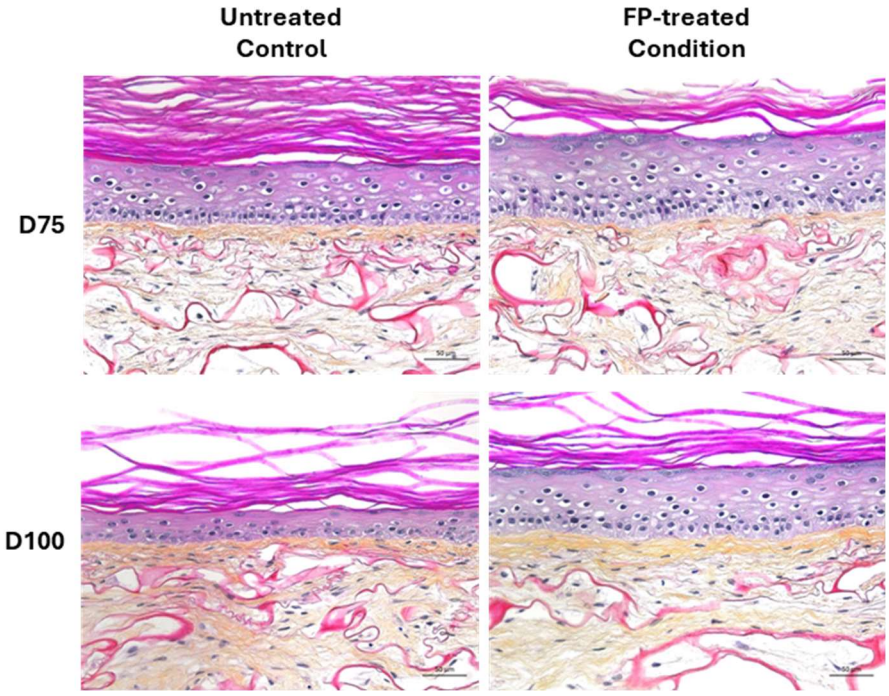

Figure 5. Histological improvement of epidermal structure following topical cosmetic treatment. HPS-stained sections of 3D SE at day 75 and day 100 comparing untreated controls and FP-treated conditions. Scale bar = 50 µm.

Additionally, immunofluorescence analysis demonstrated enhanced expression of key epidermal differentiation markers, including cytokeratin-10, filaggrin, and loricrin (Figure 6). In untreated controls, these markers were faint or discontinuous, consistent with previous

observations of ageing-associated decline. However, in FP-treated tissues, CK10 expression was restored, and both filaggrin and loricrin signals were markedly increased, with a continuous and well-organised distribution in the upper epidermis (Figure 6a). Quantitative analysis confirmed the significant upregulation of all three markers, supporting the functional recovery of the epidermal barrier (Figure 6b).

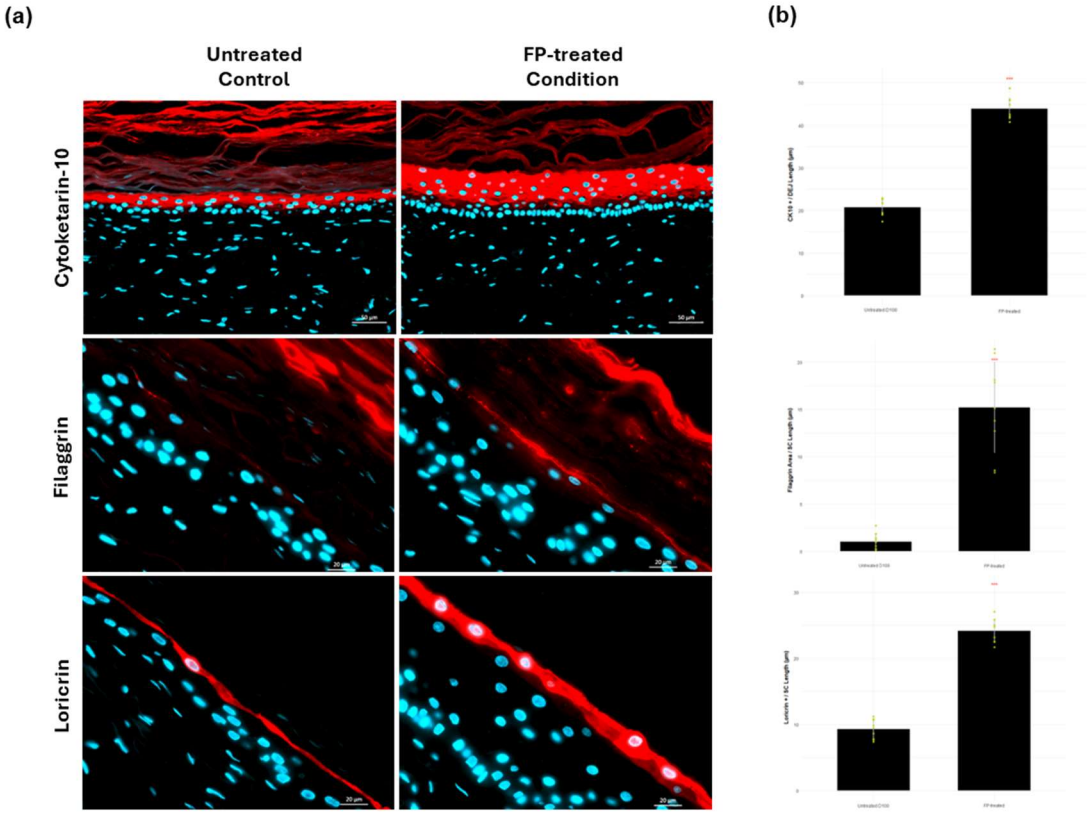

Figure 6. Topical application of the cosmetic formulation restores epidermal structure and differentiation in aged 3D SEs. (a) Representative images showing immunostaining of cytokeratin-10 (top), filaggrin (middle), and loricrin (bottom) in untreated controls and FP-treated conditions at day 100. Red: specific marker signal; blue: DAPI-stained nuclei. **(b)** Quantitative analysis of marker-positive surface area of cytokeratin-10, filaggrin, and loricrin in FP-treated SEs. Data are presented as mean ± SD. P < 0.05, P < 0.01, *P < 0.001. Scale bar = 50 µm.

Altogether, these results demonstrate that repeated topical application of the cosmetic formulation counteracts epidermal ageing by restoring both morphological thickness and molecular markers of differentiation, thereby improving epidermal homeostasis.

3.4 Cosmetic treatment restores dermal elastic matrix markers and fibre organisation

To assess whether the cosmetic formulation also exerted reparative effects on the dermal compartment, we examined the expression and organisation of fibrillin-1 and elastin in treated *versus* untreated 3D SE at days 75 and 100 (Figures 6 and 7, respectively).

In untreated controls, both fibrillin-1 and elastin showed reduced intensity and disorganised fibre networks, particularly at day 100, consistent with ageing-induced ECM degradation. In contrast, FP-treated skin equivalents displayed significantly enhanced expression of both

fibrillin-1 and elastin at both time points. The fibres appeared denser, more continuous, and more uniformly distributed beneath the dermal-epidermal junction.

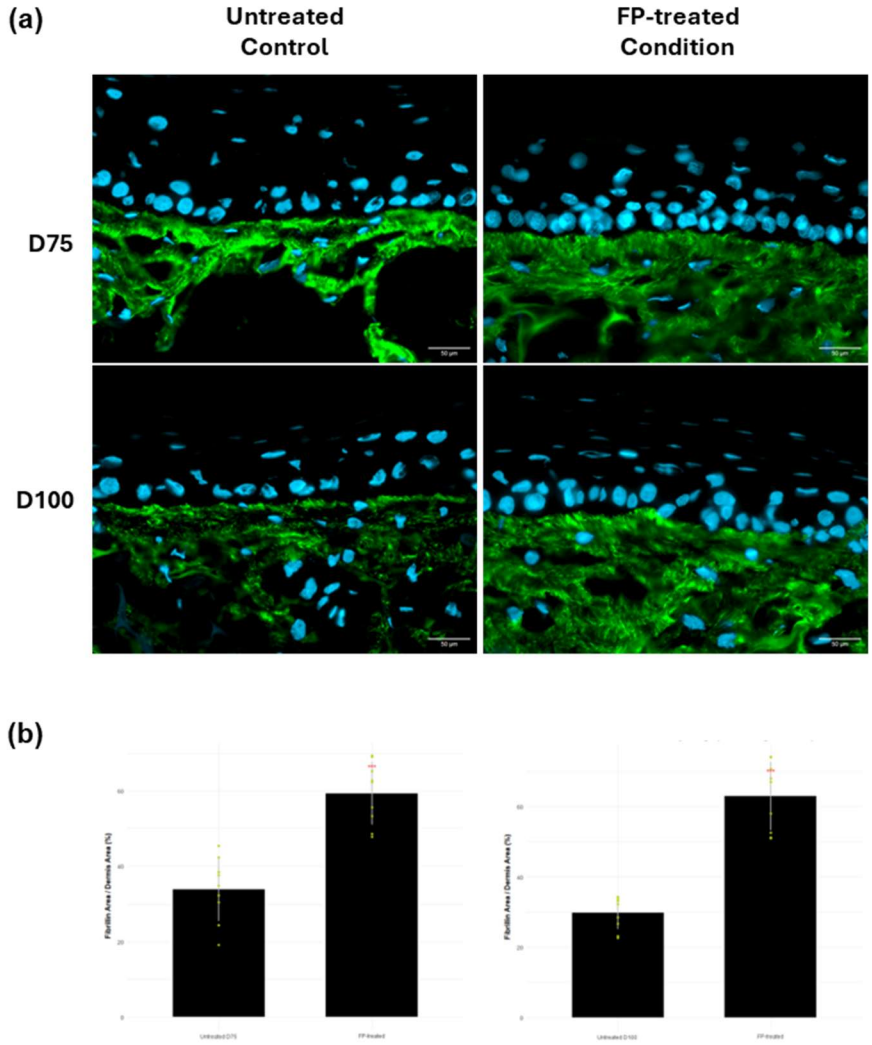

Figure 7. Topical cosmetic treatment enhances fibrillin-1 expression and fibre organisation in the dermis. (a) Confocal images showing fibrillin-1 immunostaining (green) at days 75 and 100 in untreated and FP-treated 3D skin equivalents. Nuclei are counterstained with DAPI (blue). FP treatment led to increased fibrillin-1 intensity and more continuous, well-organised fibres. **(b)** Quantification of fibrillin-1-positive area confirms a significant increase in treated tissues compared to untreated controls. Data are presented as mean ± SD. $P < 0.05$, $P < 0.01$. Scale bar = 50 µm.

Quantitative analysis confirmed this improvement: fibrillin-1 and elastin signals were significantly higher in the FP-treated group than in controls at both days 75 and 100. This suggests that repeated topical application of the cosmetic formulation not only preserves elastic matrix protein levels but also helps to maintain and restore ECM structural integrity, counteracting dermal ageing processes.

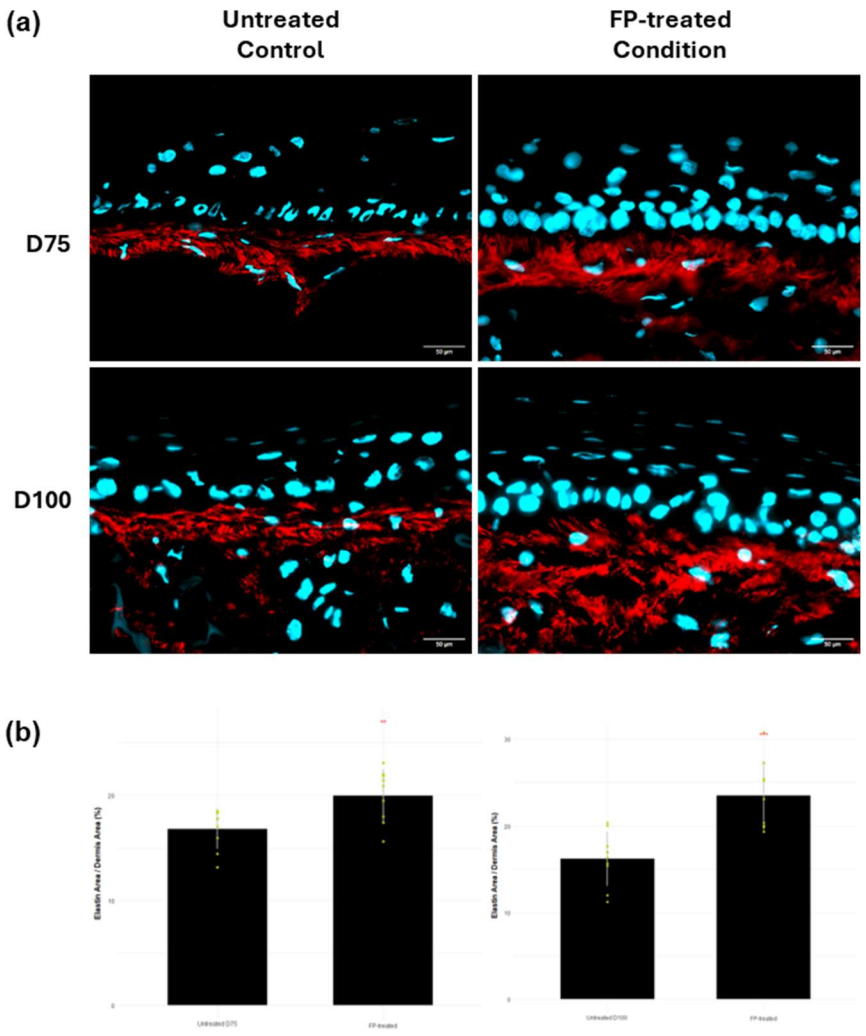

Figure 8. Repeated topical application of the cosmetic product increases elastin expression and improves dermal fibre organisation. (a) Representative images showing elastin immunostaining (red) at days 75 and 100 in untreated and FP-treated conditions. Nuclei are stained with DAPI (blue). Elastin fibres appear denser and better aligned in treated tissues. **(b)** Quantitative analysis confirms a higher elastin-positive area in FP-treated SEs. Data are presented as mean ± SD. $P < 0.05$, $P < 0.01$. Scale bar = 50 µm.

4. Discussion

After 100 days of culture, the full-thickness reconstructed skin model developed histological and molecular hallmarks of intrinsic ageing, including epidermal thinning, reduced expression of differentiation markers, and extracellular matrix (ECM) deterioration. As previously described **[2]**, this extended-time model effectively mimics the gradual, time-dependent changes associated with chronological ageing at epidermal level.

More importantly, our findings emphasise the critical role of the dermal compartment, often overlooked in short-term or epidermis-only models. Ageing in the dermis is marked not only by the downregulation of fibrillin-1 and elastin, but also by fragmentation and disorganisation of their fibre networks. These changes compromise the mechanical integrity of the skin and impair epidermal support, contributing to visible signs of ageing. Our model captured these

structural alterations over time, validating its physiological relevance and underscoring the need for dermis-inclusive platforms in ageing research.

Repeated topical application of the cosmetic product resulted in significant structural and functional restoration of the aged model. At the epidermal level, increased thickness and improved stratification were observed, alongside marked upregulation of filaggrin and loricrin, two key proteins involved in skin barrier integrity, which is often compromised during ageing **[3]**. In the dermis, enhanced expression and organisation of fibrillin-1 and elastin suggest a restructured and more functional elastic fibre network, potentially contributing to improved skin firmness and elasticity.

Developing *in vitro* ageing models remains a major challenge due to the inherently long timescale of ageing processes. Traditional models such as skin explants are limited by short viability (typically ~10 days), preventing long-term product testing. This study underscores the potential of extended-time culture models to overcome this limitation, enabling physiologically relevant, repeated topical applications over several weeks. Such systems better simulate real-life use and offer a robust alternative to short-term models for evaluating anti-ageing strategies.

5. Conclusion

Our work demonstrates, for the first time, the feasibility of using a 100-day *in vitro* full-thickness skin model to evaluate the effects of long-term repeated topical application of a cosmetic product. The model successfully mimics key features of intrinsic skin ageing and provides a predictive and realistic platform for the assessment of skincare formulations.

References

[1] Farage M, et *al*. Int J Cosmet Sci. 2008;30(2):87–95.
[2] Quan T, et *al*. Gerontology. 2015;61(5):427–34.
[3] Kohl E, et *al*. J Eur Acad Dermatol Venereol. 2011;25(8):873–84.
[4] Ponec M, et *al*. Drug Discov Today. 2002;7(14):743–53.
[5] Bell E, et *al*. Proc Natl Acad Sci U S A. 1979;76(3):1274–8.
[6] Dos Santos M, et *al*. Matrix Biol. 2015;47:85–97.
[7] Kim H, et *al*. Ann Dermatol. 2008;20(2):49–55.
[8] Piérard-Franchimont C, et *al*. Skin Res Technol. 2023;29(5):e13385.
[9] Ashapkin V, et *al*. Front Genet. 2019;10:455.
[10] Garagnani P, et *al*. J Aging Res. 2012;2012:104610.